Two-Carrier Scheme: Evading the 3 dB Quantum Penalty of Heterodyne Readout in Gravitational-Wave Detectors

Teng Zhang[©], Philip Jones[©], Jiří Smetana, Haixing Miao[©], Denis Martynov, 1 Andreas Freise, 1,2,3 and Stefan W. Ballmer,

¹School of Physics and Astronomy, and Institute of Gravitational Wave Astronomy, University of Birmingham, Edgbaston, Birmingham B15 2TT, United Kingdom

 2 Department of Physics and Astronomy, VU Amsterdam, De Boelelaan 1081, 1081 HV Amsterdam, Netherlands ³Nikhef, Science Park 105, 1098 XG Amsterdam, Netherlands ⁴Syracuse University, Syracuse, New York 13244, USA



(Received 10 August 2020; revised 6 October 2020; accepted 5 May 2021; published 1 June 2021)

Precision measurements using a traditional heterodyne readout suffer a 3 dB quantum noise penalty compared with a homodyne readout. The extra noise is caused by the quantum fluctuations in the image vacuum. We propose a two-carrier gravitational-wave detector design that evades the 3 dB quantum penalty of the heterodyne readout. We further propose a new way of realizing frequency-dependent squeezing utilizing two-mode squeezing in our scheme. It naturally achieves more precise audio frequency signal measurements with radio frequency squeezing. In addition, the detector is compatible with other quantum nondemolition techniques.

DOI: 10.1103/PhysRevLett.126.221301

Introduction.—Since 2015, laser interferometric gravitational-wave detectors have made a series of direct observations of gravitational waves from mergers of binary black holes and neutron stars [1-3]. They have opened a new observational window into the universe and provided significant inputs to many scientific fields. In the detector, to translate the electromagnetic sidebands into a measurable electrical signal, a readout scheme is required, which is also fundamental for determining the sensitivity of the detector [4].

Heterodyne readout is widely implemented in precision measurements, e.g., for the stabilization of laser frequencies and optical cavities (also known as the Pound-Drever-Hall technique [5,6]) and for quantum squeezing characterization due to its natural immunity to the lowfrequency laser noise [7–11]. Compared with homodyne readout, heterodyne readout suffers 3 dB noise penalty as the scheme picks up the vacuum fields above and below the local oscillator (LO). The additional field that does not coincide with the signal is called the image vacuum [12–15]. The noise penalty is a direct and necessary consequence of the Heisenberg uncertainty principle when all quadratures are allowed to be measured simultaneously [16]. In the first generation of gravitational wave detectors, a heterodyne readout with two balanced radio frequency (rf) sidebands was used [17], reducing the factor of 2 (3 dB) quantum penalty to a factor of 1.5. In that scheme, the vacuum fields which are twice the modulation frequency away from the carrier couple to the readout channel [16]. In subsequent detector upgrades, the readout scheme was switched to dc readout [17,18], a variant of homodyne readout. The LO in the dc readout is derived by slightly detuning the arm cavities, which offsets the interferometer from a perfect dark fringe. Direct current readout has the advantage of a straightforward implementation without needing an external LO. However, the dark-fringe offset induces extra couplings of technical noises and is not ideal for future-generation gravitational wave detectors [19]. A balanced homodyne readout can eliminate the dark fringe offset by introducing a spatially separated LO [4]. This requires auxiliary optics on the LO path and an additional output optical mode cleaner. Meanwhile, heterodyne readout is used in current detectors for the stabilization of auxiliary degrees of freedom, e.g., the lengths of recycling cavities [20,21].

Is there a way to evade the fundamental quantum noise penalty with a heterodyne readout? It was found that the noise penalty of a heterodyne readout could be evaded if the image vacuum fields can be excited to contain coherent signal flux [14,22,23]. Inspired by this finding, we give a new gravitational wave detector scheme that includes two carriers at ω_1 and ω_2 with a beam at $\omega_L = (\omega_1 + \omega_2)/2$ serving as the heterodyne LO. The three beams are evenly separated by an rf ω_m . The schematic of the design is shown in Fig. 1. The two carriers resonate, and the LO antiresonates in the arm cavities. The LO resonates in recycling cavities. This new design with a heterodyne readout will lead to the same quantum-limited sensitivity as with a homodyne readout and the same total arm power.

Another highlight of the two-carrier detector with a heterodyne readout is the simplicity of generating quantum squeezing. Most gravitational-wave signals from a compact

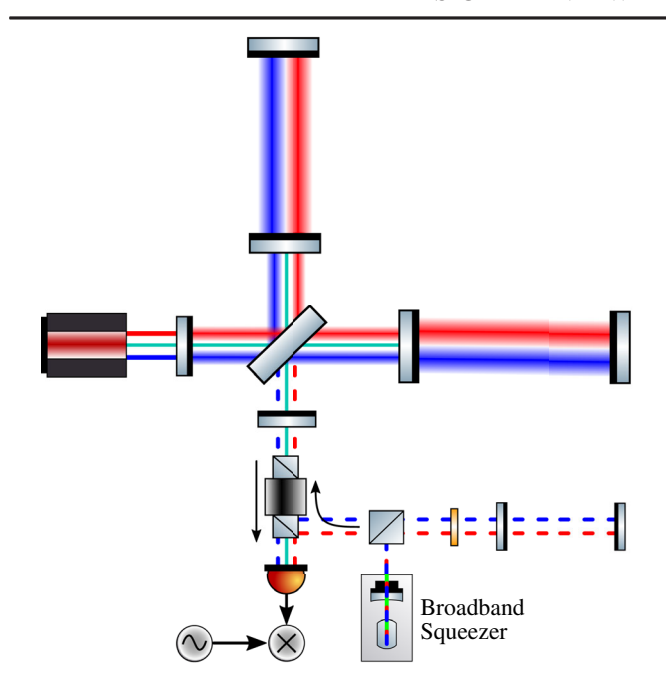


FIG. 1. Schematic of the two-carrier gravitational-wave detector with heterodyne readout. The red, blue, and cyan lasers correspond to the carriers at ω_1 , ω_2 , and the LO at $\omega_L = (\omega_1 + \omega_2)/2$, respectively. The three beams are spatially overlapped in the detector. The broadband squeezer is pumped at $2\omega_L$ and has a bandwidth from $\omega_1 - \Omega$ to $\omega_2 + \Omega$.

binary system detected by ground-based detectors are within the audio band, from several hertz to several kilohertz. However, at audio frequencies, excess noises are significant due to the parasitic interferences from scattered light [24,25]. In general, even though the signal field is on dark fringe, a bright LO is required for photon detection and can introduce audio-band scattering to the audio-band squeezer. We will show that, instead of observing audio-band squeezing [26,27] around LO frequency, radio frequency squeezing in a broadband two-mode quantum state is sufficient in our configuration, i.e., low-frequency signals measurement with high-frequency squeezing [28,29]. Note that the audio-band noises with respect to the carriers cannot be omitted.

Heterodyne readout and two-mode squeezing.—In a single sideband heterodyne readout, two vacuum fields, $\hat{s}_{1,\pm\Omega}$, $\hat{s}_{2,\pm\Omega}$ around frequencies ω_1 and ω_2 are measured as shown in Fig. 2. The eventual photocurrent containing the signal and noise can be derived as

$$I \propto \hat{s}_{1,-\Omega}^{\dagger} e^{i(\phi_L - \phi_D)} + \hat{s}_{2,-\Omega}^{\dagger} e^{i(\phi_L + \phi_D)}$$

+ $\hat{s}_{1,\Omega} e^{-i(\phi_L - \phi_D)} + \hat{s}_{2,\Omega} e^{-i(\phi_L + \phi_D)},$ (1)

where ϕ_L is the LO phase and is assumed to be $\pi/2$ in this Letter, ϕ_D is the demodulation phase. In the two-photon formalism [30,31], the photocurrent is proportional to the combined quadrature [32]

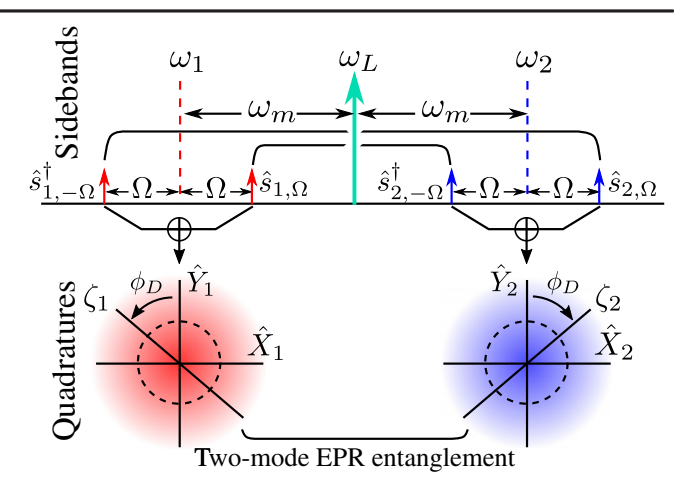


FIG. 2. Two-carrier heterodyne readout with two-mode squeezing: sideband picture (top) and quadrature picture (bottom). The two carriers are at frequencies ω_1 and ω_2 . The LO field is in the middle at $\omega_L = (\omega_1 + \omega_2)/2$. The squeezer is pumped at $2\omega_L$, entangling sideband pairs symmetric around the LO field at ω_L . This leads to a two-mode EPR entanglement between quadratures on ζ_1 and ζ_2 . Ω is audio frequency and ω_m is the separation between the LO and each carrier.

$$\hat{Q}_{\zeta} = \mathbf{H}_{\zeta} \cdot [\hat{X}_1 \quad \hat{Y}_1 \quad \hat{X}_2 \quad \hat{Y}_2]^{\mathrm{T}}, \tag{2}$$

with $\mathbf{H}_{\zeta} \equiv [\cos \zeta_1, \sin \zeta_1, \cos \zeta_2, \sin \zeta_2]$. Here, \hat{X}_j , \hat{Y}_j (j=1, 2) represent the amplitude and phase quadrature of the sidebands $\hat{s}_{1,\pm\Omega}$ and $\hat{s}_{2,\pm\Omega}$, respectively. ζ_j defines the measurement quadrature,

$$\zeta_1 = \phi_L - \phi_D, \qquad \zeta_2 = \phi_L + \phi_D. \tag{3}$$

We normalize the shot noise spectral density for the vacuum state to be 1. With the pumping laser frequency of the squeezer at $2\omega_L$, the quadratures of two modes at ω_1 and ω_2 are correlated [7,32–34], of which the correlation is quantified by the covariance matrix,

$$\mathbb{V} = \begin{bmatrix} \alpha & 0 & \beta & 0 \\ 0 & \alpha & 0 & -\beta \\ \beta & 0 & \alpha & 0 \\ 0 & -\beta & 0 & \alpha \end{bmatrix}, \tag{4}$$

where $\alpha = \cosh 2r$, $\beta = \sinh 2r$, and r is the phase squeezing factor. The spectral density of the combined quadrature \hat{Q}_{ζ} in Eq. (2) is given by

$$\mathbf{H}_{\zeta} \mathbb{V} \mathbf{H}_{\zeta}^{\mathrm{T}} = 2\alpha - 2\beta = 2e^{-2r},\tag{5}$$

which is a natural result of the EPR entanglement between quadratures of the two modes [9,35–37]. This is clearly depicted in Fig. 2. This two-mode quantum state can be achieved with a broadband squeezer, which, in principle,

gives constant squeezing within the bandwidth from $\omega_1 - \Omega$ to $\omega_2 + \Omega$. However, in our scheme, squeezing only around ω_1 and ω_2 —i.e., ω_m away from half of the squeezer pumping frequency—is required to be observed. This means that, although we need a broadband squeezer, good squeezing around ω_L is not required to be observed. In a single-carrier scheme with a heterodyne readout, in which only one of the two modes takes signal, the noise to signal ratio is $2e^{-2r}$, where the signal part is normalized to be 1. The factor of 2, here, corresponds to the well-known 3 dB quantum penalty. In the two carrier scheme, the same total power is divided into two carriers equally, and the noise to signal ratio becomes $2e^{-2r}/(\sqrt{2}/2+\sqrt{2}/2)^2=e^{-2r}$, which demonstrates the evasion of the 3 dB penalty.

Quantum noise of the detector.—So far, we have been focusing on shot noise. Inside the interferometer, the two sideband modes interact with the test mass through the radiation pressure force by beating with the two carriers, which also introduces radiation pressure noise. When the interferometer is tuned with equal power in two carriers, he optomechanical factors describing the interaction of the modes with the test mass mirrors and their cross correlation are identical. They are equal to half of the optomechanical factor $\mathcal K$ defined in Ref. [38]. Note that, here, because ω_m is much smaller than ω_j , we neglect the effect of the difference in the wavelength of two carriers. The input-output transfer matrix $\mathbb T$ for the quadratures of these two modes and their response vector $\mathbf R$ of the interferometer to the gravitational wave strain can be derived as [39]

$$\mathbb{T} = e^{2i\Phi} \begin{bmatrix} 1 & 0 & 0 & 0 \\ -\mathcal{K}/2 & 1 & -\mathcal{K}/2 & 0 \\ 0 & 0 & 1 & 0 \\ -\mathcal{K}/2 & 0 & -\mathcal{K}/2 & 1 \end{bmatrix}, \quad \mathbf{R} = \frac{e^{i\Phi}}{h_{\text{SQL}}} \begin{bmatrix} 0 \\ \sqrt{\mathcal{K}} \\ 0 \\ \sqrt{\mathcal{K}} \end{bmatrix}.$$
(6)

Here, $\Phi = \text{atan}(\Omega/\gamma)$ is the phase of the sidebands at frequency Ω acquired by reflection from the interferometer with an effective bandwidth γ . The optomechanical factor is

$$\mathcal{K} = \frac{16\omega_L P\gamma}{mcL\Omega^2(\gamma^2 + \Omega^2)},\tag{7}$$

where m is the mass of each mirror, and P is the total circulating power in the arm cavity. The standard quantum limit (SQL) of the detector in strain is $h_{\rm SOL} = \sqrt{8\hbar/(m\Omega^2L^2)}$.

The low-frequency radiation pressure noise can be improved by using frequency-dependent squeezing [38]. The filter cavity provides frequency dependent quadrature rotations θ_1 , θ_2 for the two modes, which can be described by [42]

$$\mathbb{P}_{\theta} = \begin{bmatrix} \cos \theta_1 & -\sin \theta_1 & 0 & 0\\ \sin \theta_1 & \cos \theta_1 & 0 & 0\\ 0 & 0 & \cos \theta_2 & -\sin \theta_2\\ 0 & 0 & \sin \theta_2 & \cos \theta_2 \end{bmatrix}. \tag{8}$$

The quantum noise spectral density of the heterodyne readout is given by

$$S_{hh} = \frac{\mathbf{H}_{\zeta} \mathbb{TP}_{\theta} \mathbb{VP}_{\theta}^{\mathsf{T}} \mathbb{T}^{\dagger} \mathbf{H}_{\zeta}^{\mathsf{T}}}{|\mathbf{H}_{\zeta} \mathbf{R}|^{2}}.$$
 (9)

When the frequency-dependent rotation angle satisfies

$$\cos(\theta_1 + \theta_2) = \frac{1 - \mathcal{K}^2}{1 + \mathcal{K}^2},\tag{10}$$

the noise spectrum reaches the minimal value

$$S_{hh}^{\min} = \frac{h_{\text{SQL}}^2 \mathcal{K}^2 + 1}{2} e^{-2r}.$$
 (11)

In a special case of Eq. (10), $\theta_1 = \theta_2 = \operatorname{atan} \mathcal{K}$, the required frequency dependent rotation angle is the same as that in the single-carrier detector with a homodyne readout [38]. Thus, one filter cavity is sufficient, and its parameters are identical to that in a single-carrier detector, as long as $2\omega_m$ is an integer multiple of the free spectral range (FSR) of the filter cavity. In Fig. 3, we plot the noise spectral densities

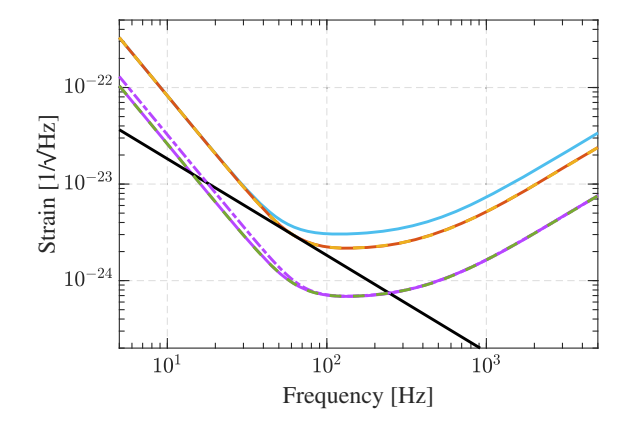


FIG. 3. Quantum-limited sensitivity of different configurations. The blue curve corresponds to the case of a single-carrier detector with heterodyne readout. The orange curve corresponds to the two-carrier detector, which perfectly overlaps with the dashed yellow curve for homodyne readout. The solid purple curve is the sensitivity of the two-carrier detector with 10 dB squeezing, which perfectly overlaps with the dashed green curve for homodyne readout with the same squeezing. The dot-dashed purple curve corresponds to a 15% power imbalance between the two carriers while the total power stays constant. The black curve is the standard quantum limit. The detector and filter cavity parameters used in the two-carrier detector are the same as those of Advanced LIGO [43,44] and Advanced LIGO upgrade [45].

for different configurations as a comparison. The two-carrier detector with a heterodyne readout gives identical sensitivity to that of Advanced LIGO with a homodyne readout. The figure also shows that the scheme is robust against a power imbalance between the two carriers. A rather large 15% power imbalance between the two carriers under 10 dB frequency-dependent squeezing only results in a 20% degradation in sensitivity at low frequencies. At low frequencies, where the radiation pressure noise dominates, an ideal EPR measurement at the output of the interferometer is not enabled due to an asymmetric optomechanical effect from the power imbalance. The impact of a 15% power imbalance on the signal is negligible, leading to only a 0.57% sensitivity degradation at high frequencies.

Criteria for macroscopic lengths.—In our proposed scheme, the lengths between core optics need to be carefully set to defined absolute values to guarantee coresonance of the respective optical fields. This introduces requirements on the macroscopic lengths in addition to the usual requirements for controlling the microscopic position of the optics. We anticipate this coresonance requirement to be relatively easy to achieve, as the current lock acquisition system already permits selecting a specific fringe.

To keep the carriers resonant and the LO beam antiresonant in the arm cavities, $2\omega_m$ shall be an odd multiple of the FSR of the arm cavity. Another consideration is on the coupling between the symmetric and antisymmetric ports for both the carriers and the LO. Taking the LO field as dc by convention ($\omega_L = 0$, $\omega_1 = -\omega_m$, $\omega_2 = \omega_m$), and locking the central Michelson on its bright fringe, we can treat the central Michelson as an effective mirror with amplitude transmissivity

$$r_{\rm MI} = i r_a \sin \frac{\omega \Delta l}{c}, \qquad t_{\rm MI} = r_a \cos \frac{\omega \Delta l}{c}, \qquad (12)$$

where ω is the sideband frequency, Δl is the Schnupp asymmetry [21], and r_a is the amplitude reflectivity of arm cavities. For the LO antiresonating in the arm cavities, $r_a = -1$, and $\omega = \omega_L = 0$. For the carriers we have $r_a = 1$, as well as $\omega = \omega_1 = -\omega_m$ and $\omega = \omega_2 = \omega_m$, respectively. To keep the carriers on the Michelson dark fringe, we need to have $\omega_m \Delta l/c = \pi/2$. The macroscopic round-trip length of the signal recycling cavity and power recycling cavity should be tuned to satisfy the following conditions: in the signal recycling cavity, the signal (carrier) modes are antiresonant, while the LO beam is resonant; in the power recycling cavity, all three beams are on resonance. In Advanced LIGO, ω_m is around $2\pi \times 45$ MHz, so Δl needs to be around 1.67 m. Given the Advanced LIGO power and signal recycling mirror transmissivities of 0.03 and 0.325, the effective power transmissivity of the LO field from the symmetric port to the antisymmetric port is around 25%. To use one filter cavity for two modes, we can make $2\omega_m$ be an integer multiple of the FSR of the filter cavity, as mentioned earlier.

The mirror motion coupling at $2\omega_m$.—With two carriers resonating in the arm cavities, the mirror motion around $2\omega_m$ sensed by one carrier is also measured within the audio band with respect to other carriers. The additional noise current is

$$I_{2\omega_{m}} \propto \hat{s}_{1,2\omega_{m}-\Omega}^{\dagger} e^{i(\phi_{L}+\phi_{D})} + \hat{s}_{2,-2\omega_{m}-\Omega}^{\dagger} e^{i(\phi_{L}-\phi_{D})} + \hat{s}_{1,2\omega_{m}+\Omega} e^{-i(\phi_{L}+\phi_{D})} + \hat{s}_{2,-2\omega_{m}+\Omega} e^{-i(\phi_{L}-\phi_{D})}, \quad (13)$$

where $\phi_L = \pi/2$, $\phi_D = 0$ in our scheme. Around frequency $2\omega_m$, the radiation pressure also excites mirror motion at the vibration mode resonances of the mirror. The susceptibility at $2\omega_m + \Omega$ of the vibration mode at resonant frequency ω_a can be modeled as a harmonic oscillator with the damping part described by mechanical dispersion, ψ ($\psi = 1/Q$, Q is the quality factor), as [46]

$$\chi_a = \frac{1}{\mu m [\omega_a^2 + i\omega_a^2 \psi - (2\omega_m + \Omega)^2]},$$
 (14)

where μ is an effective mass coefficient which includes the coupling between mirror mode and the carrier Gaussian mode.

In order to not affect the quantum sensitivity, we need the radiation pressure induced mirror motion around $2\omega_m$ to be much smaller than the quantum shot noise. In other words, $|\chi_a|$ need to be much smaller than the absolute value of the free mass susceptibility, $1/(m\Omega^2)$, at a frequency where radiation pressure noise is approximate to shot noise. For $\omega_a = 2\omega_m + \Omega$, and taking $\Omega = 2\pi \times 60$ Hz, L = 4 km, $\omega_m \approx 2\pi \times 45$ MHz, this requires

$$\frac{Q}{\mu} \ll 2.25 \times 10^{12}$$
. (15)

Around 90 MHz, the Q of silica is around 10^5 [47]. We use program, CYPRES [48] and simulate the effective mass coefficients up to 300 kHz taking Advanced LIGO mirror and beam size as the example. As it turns out, μ is always larger than 0.1 without observing a trend of smaller μ toward higher frequency. Details are in the Supplemental Material [39]. It proves the satisfaction of Eq. (15) indirectly.

The thermal noise at 90 MHz from the mode at the same frequency can be calculated as [46]

$$\sqrt{S_{th}} = \sqrt{4 \times \frac{4k_B T Q}{\mu m \omega_a^3 L^2}}$$

$$= 2.4 \times 10^{-25} \sqrt{\frac{T}{300 \text{ K}} \times \frac{1}{\mu} \times \frac{Q}{10^5} \frac{1}{\sqrt{\text{Hz}}}}, \quad (16)$$

with a bandwidth around $\omega_a/(2\pi Q)=900$ Hz. k_B is the Boltzmann constant, T is the environment temperature. From the mode simulation (with details in Supplemental Material [39]), we observe that the density of modes with μ no larger than 1 is almost constant over frequency and around one mode per 2.5 kHz on average. Even though assuming that the mode separation is the same as the mode bandwidth, the thermal noise at 90 MHz results $3.1\times10^{-25}(1/\sqrt{\rm Hz})$, by taking contributions from 100 modes in the vicinity into account. The thermal noise is compatible with the quantum noise of the two-carrier detector, but experimental studies with more details are required in the future.

Conclusions and discussion.—We have shown that the proposed two-carrier gravitational wave detector with heterodyne readout evades the 3 dB quantum penalty of a conventional heterodyne readout. It also allows the usage of two-mode squeezing in the same way of single mode squeezing with a homodyne readout. Furthermore, the twocarrier detector provides advantages: (1) it can enable squeezing enhanced measurements in the audio band and below with high-frequency squeezing, which is immune to the audio-band LO scattering contamination to the squeezer, although still susceptible to the scattering from residual carriers; (2) it allows us to operate the interferometer on the dark fringe without an additional LO path and output mode cleaners that are essential to the balanced homodyne readout scheme, in which two mode cleaners are required [32]. If the higher optical modes at the dark port cannot be suppressed by the interferometer itself, one output mode cleaner, of which the FSR equals to ω_m , is sufficient.

As an outlook, we want to highlight that the two-carrier detector is compatible with general quantum nondemolition schemes [49,50], in contrast to a conventional heterodyne readout [16]. For example, similar to the implementation of frequency dependent squeezing, we can add a filter cavity at the output to realize a frequency-dependent readout for back action evasion [38]. The resulting optimal sensitivity is

$$S_{hh}^{\text{opt}} = \frac{h_{\text{SQL}}^2}{2} \frac{1}{\mathcal{K}} e^{-2r}.$$
 (17)

This saturates the fundamental quantum limit or the quantum Cramér-Rao bound [51–54].

We acknowledge the support from simulation software, FINESSE and Francois Bondu for providing the simulation program, CYPRES. T. Z., P. J., H. M., D. M., and A. F. acknowledge the support of the Institute for Gravitational Wave Astronomy at University of Birmingham. A. F. has been supported by a Royal Society Wolfson Fellowship which is jointly funded by the Royal Society and the Wolfson Foundation. H. M. is supported by UK STFC Ernest Rutherford Fellowship

(Grant No. ST/M005844/11). S. W. B. acknowledges the supported by the National Science Foundation Grant No. PHY-1912536. This document was assigned the LIGO document control number LIGO-P2000260.

- [1] B. Abbott, R. Abbott, T. Abbott, M. Abernathy, F. Acernese, K. Ackley, C. Adams, T. Adams, P. Addesso, R. Adhikari et al. (LIGO Scientific and Virgo Collaborations), Observation of Gravitational Waves from a Binary Black Hole Merger, Phys. Rev. Lett. 116, 061102 (2016).
- [2] B. Abbott, R. Abbott, T. Abbott, M. Abernathy, F. Acernese, K. Ackley, C. Adams, T. Adams, P. Addesso, R. Adhikari et al. (LIGO Scientific and Virgo Collaborations), Gw170817: Observation of Gravitational Waves from a Binary Neutron Star Inspiral, Phys. Rev. Lett. 119, 161101 (2017).
- [3] B. Abbott, R. Abbott, T. Abbott, M. Abernathy, F. Acernese, K. Ackley, C. Adams, T. Adams, P. Addesso, R. Adhikari et al. (LIGO Scientific and Virgo Collaborations), Gwtc-1: A Gravitational-Wave Transient Catalog of Compact Binary Mergers Observed by LIGO and Virgo during the First and Second Observing Runs, Phys. Rev. X 9, 031040 (2019).
- [4] P. Fritschel, M. Evans, and V. Frolov, Balanced homodyne readout for quantum limited gravitational wave detectors, Opt. Express **22**, 4224 (2014).
- [5] R. W. P. Drever, J. L. Hall, F. V. Kowalski, J. Hough, G. M. Ford, A. J. Munley, and H. Ward, Laser phase and frequency stabilization using an optical resonator, Appl. Phys. B 31, 97 (1983).
- [6] E. D. Black, An introduction to Pound-Drever-Hall laser frequency stabilization, Am. J. Phys. 69, 79 (2001).
- [7] J. Gea-Banacloche and G. Leuchs, Squeezed states for interferometric gravitational-wave detectors, J. Mod. Opt. 34, 793 (1987).
- [8] V. Chickarmane, S. V. Dhurandhar, T. C. Ralph, M. Gray, H.-A. Bachor, and D. E. McClelland, Squeezed light in a frontal-phase-modulated signal-recycled interferometer, Phys. Rev. A 57, 3898 (1998).
- [9] A. M. Marino, J. C. R. Stroud, V. Wong, R. S. Bennink, and R. W. Boyd, Bichromatic local oscillator for detection of two-mode squeezed states of light, J. Opt. Soc. Am. B 24, 335 (2007).
- [10] W. Li, X. Yu, and J. Zhang, Measurement of the squeezed vacuum state by a bichromatic local oscillator, Opt. Lett. 40, 5299 (2015).
- [11] S. Feng, D. He, and B. Xie, Quantum theory of phasesensitive heterodyne detection, J. Opt. Soc. Am. B 33, 1365 (2016).
- [12] S. D. Personick and B. S. T. F. Brief, An image band interpretation of optical heterodyne noise, Bell Syst. Tech. J. 50, 213 (1971).
- [13] H. P. Yuen and V. W. S. Chan, Noise in homodyne and heterodyne detection, Opt. Lett. 8, 177 (1983).
- [14] M. Collett, R. Loudon, and C. Gardiner, Quantum theory of optical homodyne and heterodyne detection, J. Mod. Opt. 34, 881 (1987).

- [15] C. M. Caves and P. D. Drummond, Quantum limits on bosonic communication rates, Rev. Mod. Phys. 66, 481 (1994).
- [16] A. Buonanno, Y. Chen, and N. Mavalvala, Quantum noise in laser-interferometer gravitational-wave detectors with a heterodyne readout scheme, Phys. Rev. D 67, 122005 (2003).
- [17] S. Hild, H. Grote, J. Degallaix, S. Chelkowski, K. Danzmann, A. Freise, M. Hewitson, J. Hough, H. Lck, M. Prijatelj, K. A. Strain, J. R. Smith, and B. Willke, DC-readout of a signal-recycled gravitational wave detector, Classical Quantum Gravity 26, 055012 (2009).
- [18] T. T. Fricke, N. D. Smith-Lefebvre, R. Abbott, R. Adhikari, K. L. Dooley, M. Evans, P. Fritschel, V. V. Frolov, K. Kawabe, J. S. Kissel, B. J. J. Slagmolen, and S. J. Waldman, DC readout experiment in enhanced LIGO, Classical Quantum Gravity 29, 065005 (2012).
- [19] H. Yu, D. Martynov, S. Vitale, M. Evans, D. Shoemaker, B. Barr, G. Hammond, S. Hild, J. Hough, S. Huttner, S. Rowan, B. Sorazu, L. Carbone, A. Freise, C. Mow-Lowry, K. L. Dooley, P. Fulda, H. Grote, and D. Sigg, Prospects for Detecting Gravitational Waves at 5 hz with Ground-Based Detectors, Phys. Rev. Lett. 120, 141102 (2018).
- [20] M. A. Arain and G. Mueller, Design of the advanced ligo recycling cavities, Opt. Express **16**, 10018 (2008).
- [21] K. Izumi and D. Sigg, Advanced LIGO: Length sensing and control in a dual recycled interferometric gravitational wave antenna, Classical Quantum Gravity 34, 015001 (2017).
- [22] H. Fan, D. He, and S. Feng, Experimental study of a phasesensitive heterodyne detector, J. Opt. Soc. Am. B 32, 2172 (2015).
- [23] J.-B. Béguin, E. M. Bookjans, S. L. Christensen, H. L. Sørensen, J. H. Müller, E. S. Polzik, and J. Appel, Generation and Detection of a Sub-Poissonian Atom Number Distribution in a One-Dimensional Optical Lattice, Phys. Rev. Lett. 113, 263603 (2014).
- [24] H. Vahlbruch, S. Chelkowski, K. Danzmann, and R. Schnabel, Quantum engineering of squeezed states for quantum communication and metrology, New J. Phys. 9, 371 (2007).
- [25] S. S. Y. Chua *et al.*, Impact of backscattered light in a squeezing-enhanced interferometric gravitational-wave detector, Classical Quantum Gravity 31, 035017 (2014).
- [26] J. Abadie, B. P. Abbott, R. Abbott, T. D. Abbott *et al.* (LIGO Scientific Collaboration), A gravitational wave observatory operating beyond the quantum shot-noise limit, Nat. Phys. 7, 962 (2011).
- [27] J. Aasi, J. Abadie, B. P. Abbott, R. Abbott, T. D. Abbott, M. R. Abernathy *et al.* (LIGO Scientific Collaboration), Enhanced sensitivity of the LIGO gravitational wave detector by using squeezed states of light, Nat. Photonics 7, 613 (2013).
- [28] Z. Zhai and J. Gao, Low-frequency phase measurement with high-frequency squeezing, Opt. Express **20**, 18173 (2012).
- [29] W. Li, Y. Jin, X. Yu, and J. Zhang, Enhanced detection of a low-frequency signal by using broad squeezed light and a bichromatic local oscillator, Phys. Rev. A **96**, 023808 (2017).

- [30] C. M. Caves and B. L. Schumaker, New formalism for two-photon quantum optics. I. Quadrature phases and squeezed states, Phys. Rev. A **31**, 3068 (1985).
- [31] B. L. Schumaker and C. M. Caves, New formalism for twophoton quantum optics. II. Mathematical foundation and compact notation, Phys. Rev. A 31, 3093 (1985).
- [32] T. Zhang, D. Martynov, A. Freise, and H. Miao, Quantum squeezing schemes for heterodyne readout, Phys. Rev. D **101**, 124052 (2020).
- [33] J. Zhang, Einstein-Podolsky-Rosen sideband entanglement in broadband squeezed light, Phys. Rev. A 67, 054302 (2003).
- [34] R. Schnabel, Squeezed states of light and their applications in laser interferometers, Phys. Rep. **684**, 1 (2017).
- [35] Y. Ma, H. Miao, B. H. Pang, M. Evans, C. Zhao, J. Harms, R. Schnabel, and Y. Chen, Proposal for gravitational-wave detection beyond the standard quantum limit through EPR entanglement, Nat. Phys. 13, 776 (2017).
- [36] S. L. Danilishin, F. Y. Khalili, and H. Miao, Advanced quantum techniques for future gravitational-wave detectors, Living Rev. Relativity **22**, 2 (2019).
- [37] J. Sdbeck, S. Steinlechner, M. Korobko, and R. Schnabel, Demonstration of interferometer enhancement through Einstein–Podolsky–Rosen entanglement, Nat. Photonics 14, 240 (2020).
- [38] H. J. Kimble, Y. Levin, A. B. Matsko, K. S. Thorne, and S. P. Vyatchanin, Conversion of conventional gravitational-wave interferometers into quantum nondemolition interferometers by modifying their input and/or output optics, Phys. Rev. D 65, 022002 (2001).
- [39] See Supplemental Material at http://link.aps.org/supplemental/10.1103/PhysRevLett.126.221301 for detailed derivations, which includes Refs. [40,41].
- [40] H. Rehbein, H. Müller-Ebhardt, K. Somiya, S. L. Danilishin, R. Schnabel, K. Danzmann, and Y. Chen, Double optical spring enhancement for gravitational-wave detectors, Phys. Rev. D 78, 062003 (2008).
- [41] A. Buonanno and Y. Chen, Scaling law in signal recycled laser-interferometer gravitational-wave detectors, Phys. Rev. D **67**, 062002 (2003).
- [42] S. L. Danilishin and F. Y. Khalili, Quantum measurement theory in gravitational-wave detectors, Living Rev. Relativity 15, 5 (2012).
- [43] J. Aasi, B. P. Abbott, R. Abbott, T. Abbott, M. R. Abernathy, K. Ackley, C. Adams, T. Adams, P. Addesso, R. X. Adhikari et al. (LIGO Scientific Collaboration), Advanced LIGO, Classical Quantum Gravity 32, 074001 (2015).
- [44] L. McCuller, C. Whittle, D. Ganapathy, K. Komori, M. Tse, A. Fernandez-Galiana, L. Barsotti, P. Fritschel, M. MacInnis, F. Matichard, K. Mason, N. Mavalvala, R. Mittleman, H. Yu, M. E. Zucker, and M. Evans, Frequency-Dependent Squeezing for Advanced LIGO, Phys. Rev. Lett. 124, 171102 (2020).
- [45] L. Barsotti, L. McCuller, M. Evans, and P. Fritschel, The a + design curve, LIGO Document T1800042, 2018.
- [46] A. Gillespie and F. Raab, Thermally excited vibrations of the mirrors of laser interferometer gravitational-wave detectors, Phys. Rev. D 52, 577 (1995).

- [47] J. Wiedersich, S. V. Adichtchev, and E. Rössler, Spectral Shape of Relaxations in Silica Glass, Phys. Rev. Lett. 84, 2718 (2000).
- [48] F. Bondu and J.-Y. Vinet, Mirror thermal noise in interferometric gravitational-wave detectors, Phys. Lett. A **198**, 74 (1995).
- [49] V. B. Braginsky, Y. I. Vorontsov, and K. S. Thorne, Quantum nondemolition measurements, Science 209, 547 (1980).
- [50] Y. Chen, S. L. Danilishin, F. Y. Khalili, and H. Mller-Ebhardt, QND measurements for future gravitational-wave detectors, Gen. Relativ. Gravit. 43, 671 (2011).
- [51] C. Helstrom, Minimum mean-squared error of estimates in quantum statistics, Phys. Lett. 25A, 101 (1967).
- [52] V. B. Braginsky, M. L. Gorodetsky, F. Y. Khalili, and K. S. Thorne, Energetic quantum limit in large-scale interferometers, AIP Conf. Proc. **523**, 180 (2000).
- [53] M. Tsang, H. M. Wiseman, and C. M. Caves, Fundamental Quantum Limit to Waveform Estimation, Phys. Rev. Lett. 106, 090401 (2011).
- [54] H. Miao, R. X. Adhikari, Y. Ma, B. Pang, and Y. Chen, Towards the Fundamental Quantum Limit of Linear Measurements of Classical Signals, Phys. Rev. Lett. 119, 050801 (2017).